

Study on the Corrosion Behavior of 7A52 Al Alloy Welded Joint by Electrochemical Method

Chao Yang^{1,2}, Weimin Guo^{1,*}, Huixia Zhang¹, Ri Qiu¹, Jian Hou¹, Yubin Fu^{2,*}

¹ State key laboratory for marine corrosion and protection, Luoyang Ship Material Research Institute, Qingdao 266101, China

² Institute of Materials Science and Engineering, Ocean University of China, Qingdao 266100, China

*E-mail: ffyybb725@vip.sina.com; guowm@sunrui.net

Received: 3 May 2013 / Accepted: 9 June 2013 / Published: 1 July 2013

Twin-wire metal inert gas arc welding (TMW) was used to join the 7A52 Al alloy plates with the ER 5356 filler. The microstructure observation showed that the joint included four zones, i. e., base metal, heat affected zone, fusion zone and weld zone. The observations demonstrated the development of crystal structure of the four parts with four different grain sizes. Corrosion behavior of the four parts in seawater was investigated by electrochemical methods. The result indicated that elements distribution and microstructure made the electrochemical behavior different. Fusion zone had the best corrosion resistance. However, heat affected zone and weld zone are more susceptible to corrode within 80 h. In the late immersion stage, the three zones including base metal, weld zone and heat affected zone will behave similarly to the corrosion environment.

Keywords: Twin-wire metal inert gas arc welding; 7A52 Al alloy; electrochemical; corrosion

1. INTRODUCTION

A large number of aluminum alloy plates, which are mainly used as the decks, the shell plates and the cabin reinforcing plates, are applied in the design and construction of the ships. 7A52 high strength aluminum alloy and its weldment are widely utilized in shipbuilding engineering due to the high specific strength, good fracture toughness, low cycle fatigue properties and easy-welding properties. In the practical engineering activity, welding plays essential role to join the different parts together [1]. The final properties of the welded joint are attributed to the welding procedures, welding methods and solder wire. Many welding methods, such as metal inert gas arc welding (MIG), argon tungsten-arc welding (TIG) and friction stir welding (FSW), are applied to the 7A52 aluminum alloy welding. At present, its plate is mainly used by MIG. However, the conventional single-wire metal

inert gas arc welding of 7A52 Al alloy plates commonly causes the issues of coarsening and puckering due to high heat input welding, which deteriorates its mechanical properties and leads to high stress corrosion cracking (SCC) susceptibility. The technology of twin-wire metal inert gas arc welding (TMW) would meet the requirements of arc control through adjusting the welding parameters and forming a unified weld puddle, which results a preferable welding joint. Unfortunately, aluminum alloy plates of ships have to expose in the corrosive marine environment for long time, which makes the joint susceptible to the localized corrosive attacks, such as pitting corrosion, intergranular corrosion and SCC [2-3]. Welding often makes this situation worse, owing to the metallurgical changes and residual stresses introduced [4-5]. Therefore, it is of great significance to research the corrosion behavior of Al alloy welding joint in seawater.

Currently, corrosion failure research of Al alloy weldment mainly focuses on SCC susceptibility [6-7], while the discussion on electrochemical behaviors seems rare [8-9]. In our previous study, SCC behavior of the parent material and the welded specimens was investigated by the slow strain rate tensile (SSRT) test method [10]. It was found that the welded specimens exhibited higher SCC susceptibility than the parent materials by SSRT testing in seawater. In order to study the electrochemical corrosion behavior of the weldment in detail, the microstructure and electrochemical characteristic of the base metal (BM), heat affected zone (HAZ), fusion zone (FZ) and weld zone (WZ) of the TMW 7A52 Al alloy joint were discussed in this work. Conventional metallography test was used to obtain information of microstructure, which could provide reference for electrochemical analysis. Element distribution of the different zones is also an important factor affecting the electrochemical behavior. Based on this, potentiodynamic polarization curves and electrochemical impedance spectroscopy (EIS) were conducted to investigate the localized corrosion behaviour of TMW joint.

2. EXPERIMENTAL PROCEDURES

Table 1. The chemical composition of 7A52 Al alloy and ER5356 filler

	Al	Zn	Mg	Cu	Mn	Cr	Ti	Zr	Fe
7A52	Bal.	4.0~4.8	2.0~2.8	0.20~0.5	0.20~0.5	0.15~0.25	0.05~0.18	0.05~0.15	0.30
5356	Bal.	0.10	4.5~5.5	0.1	0.05~0.2	0.05~0.2	0.06~0.2		

Table 2. The welding parameters of TMW(p1 Host parameters; p2 Auxiliary parameter)

	Level I		Level II		Level III	
	P1	P2	P1	P2	P1	P2
welding voltage/ V	22	20	22	20	22	20
welding current/ A	240	190	240	192	240	195
welding speed/ cm/min	40	40	35	35	35	35
wire feeding speed m/min	9-11	8-10				
interpass temperature/ °C	70-80	70-80	70-80	70-80		

7A52 Al alloy plate (minimum yield strength 445 MPa) welded with an ER5356 filler wire was used for this investigation. The chemical composition of 7A52 Al alloy and ER5356 filler wire are given in Table 1. The welding parameters of TMW are showed in Table 2.

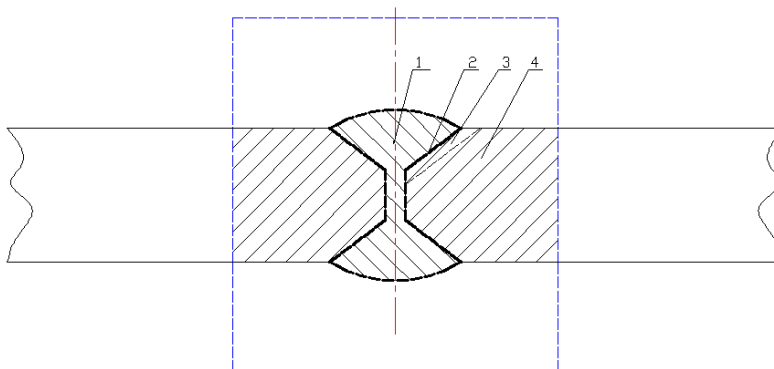


Figure 1. The schematic illustration of welding joint:(1) weld zone, (2) fusion zone, (3)heat affected zone and (4) base metal.

For the macro-/microstructural analysis, the welded joint was polished by conventional metallography approach and etched in Flick's reagent for 45 s. The specimens obtained from the four zones are schematically illustrated as Fig. 1. For electrochemical tests, the samples were polished with #2000 emery paper and cleaned with acetone. After that, those specimens were mounted in silica gel, leaving an exposed area of 2.5 cm². A typical three electrode system consisting of the specimen as the working electrode, Pt/Nb wire ($\Phi=2$ mm) as the counter electrode and saturated calomel electrode (SCE) as a reference electrode were used in the study. The nature seawater was used as electrolyte during the electrochemical measurements. Potentiodynamic polarization plots were obtained at a scanning rate of 1 mV/s from open circuit potential using electrochemical workstation (PARSTAT 2273). Impedance spectra were collected at the open circuit potential with the amplitude of 10 mV, using the frequency ranging from 100 kHz to 0.01 Hz. Fitting of impedance spectra was realized by using Zview software (Scribner Associates, Inc.). The macro-surfaces of specimens immersed in seawater for 200 h were observed by optical microscope and elements distribution on the surface detected by energy-dispersive X-ray fluorescence analysis (EDX).

3. RESULTS AND DISCUSSION

Microstructural features of welded joint of 7A52 Al alloy are showed in Fig. 2. Banded grains can be seen in the BM as shown in Fig. 2a. The WZ revealed fine grain size and the uniform distribution of secondary phase particles due to high speed welding and low heat input during process of welding, as shown in Fig. 2d. Slightly smaller equiaxial grains are observed in the HAZ just outside the FZ due to recrystallization, as shown in Fig. 2b. However, the FZ (Fig. 2c) exhibits cylindrical grains along heat dissipation.

Table 3. EDX of WZ(a), FZ & HAZ (b) of TMW 7A52 Al alloy welded joint

Element	Mg		Al		Zn	
	Wt%	At%	Wt%	At%	Wt%	At%
WZ	05.51	06.13	93.02	93.26	01.46	00.61
FZ&TMAZ	02.75	03.11	94.02	95.54	03.23	01.35

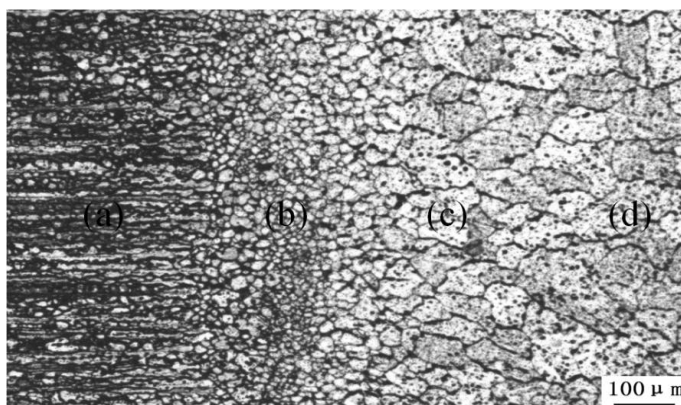


Figure 2. Optical micrograph of (a) base metal, (b) heat-affected zone,(c) fusion zone,(d)weld zone of TMW 7A52 Al alloy joint

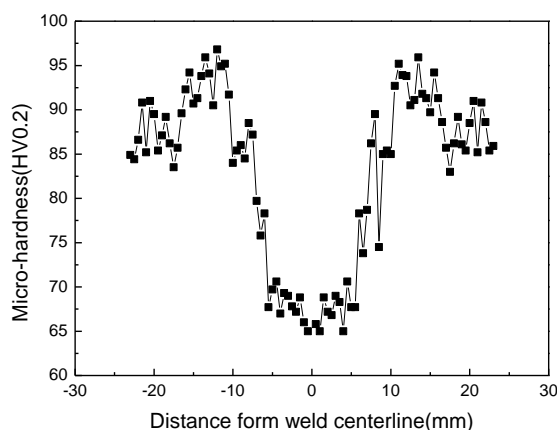


Figure 3. Vickers hardness values as measured across the TMW 7A52 Al sample with 0.5 indent spacing.

Fig. 3 shows Vickers hardness values measured across the welded joint. The Vickers hardness of the welding region demonstrates the “M” shaped hardness distribution characteristic. The hardness minima in the WZ are a result of the content of Zn that is 1.46 % in the WZ which can be seen from the EDX as shown in Table.3, that is lower than that in FZ, TMAZ and BM (Table 1, 4.0~4.8%, by weight). According to a research work, the decrease of zinc, which makes up the strengthening phase β -MgZn₂, is the important reason for the loss in mechanical properties of WZ. The increase of Zn (1.46% in WZ, 3.23% in FZ and TMAZ, 4.0~4.8% in BM) finally leads to the hardness raise from WZ

to BM. It can also be observed that a slight decrease in the hardness values of BM compared with HAZ. It is because that the HAZ has the smaller equiaxial grains and the higher dislocation density due to recrystallization [11].

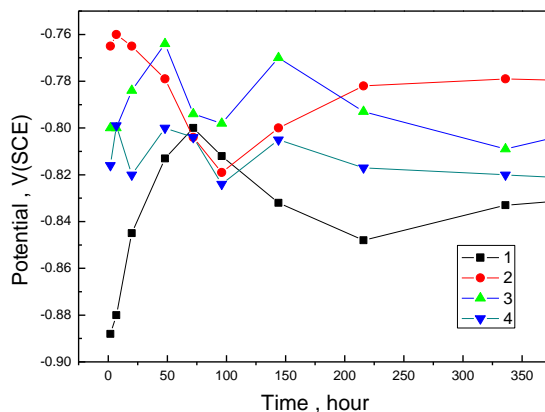


Figure 4. Variation of seawater corrosion potential of TMW 7A52 Al alloy joint.(1) BM, (2) WZ, (3) FZ, (4) HAZ.

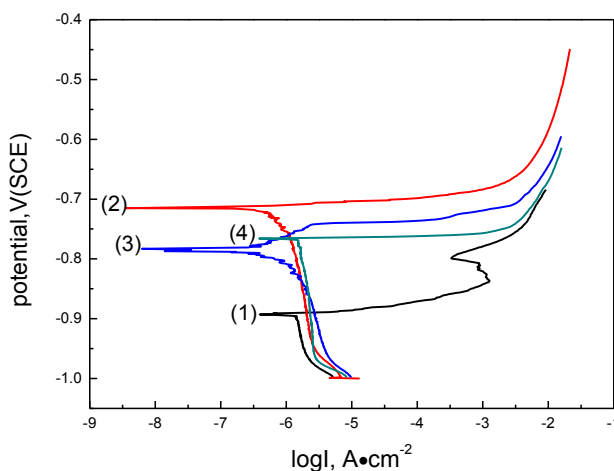


Figure 5. Potentiodynamic polarization curves for TMW 7A52 Al alloy specimens: (1) BM, (2) WZ, (3) FZ ,(4) HAZ.

Fig. 4 depicts the open circuit potential (OCP) of the TMW specimens immersed in nature seawater from 0 h to 350 h. In Fig. 4, the potentials of BM (curve 1) are initially very negative (-0.89 V). They varied rapidly within 50 h, and gradually from 50 h to 125 h. After 125 h, the potentials of all specimens mainly became stable (-0.83 V for BM, -0.78 V for WZ, -0.80 V for FZ,-0.82 V for HAZ). The environment factors strongly affect corrosion potential of metals while micro-structural change in aluminum alloys usually causes an appreciable shift on their corrosion potential in the saline solution [12]. Theoretically, there will be a larger potential difference between BM and WZ, which can form an

obvious galvanic corrosion apparently. However, oxide film on the surface of BM makes the trend weak.

The welding process of 7A52 Al alloy inevitably leads to a variety of microstructure changes that characterize different corrosion potentials. Therefore, the mechanical capacity and electrochemical corrosion behavior of TMW specimens, governed by welding process, may correlate with the changes that directly reflected by the corrosion potentials. The abrupt shift from -0.89 to -0.80 V (for BM) within 80 h is worth noticing.

For alloys, the polarization plots are quite unsymmetrical for passive metals (Fig. 5) [13]. The cathodic branch begins with oxygen diffusion control reduction, followed by hydrogen reduction below -1 V. The anodic branch starts with a rapid increase of current and a limiting current was observed in seawater. The BM showed passivation behavior with a dramatic decrease in the current density. The current density of BM decreased due to the formation of a thin oxide film of boehmite ($\text{Al}_2\text{O}_3 \cdot \text{H}_2\text{O}$), which could weaken the anodic dissolution of Al [14]. The curves indicated that the passive potential range of the FZ extended 230 mV before pitting corrosion occurred. However, HAZ and WZ of the joint had practically no corrosion resistance and pitting corrosion occurred immediately without any passivity region. It explains that the corrosion resistances of BM and FZ are higher than WZ and HAZ. The key reason for the high corrosion susceptibility is the existence of the numerical welding defects in the WZ and a higher dislocation density in the HAZ due to recrystallization. Table 4 shows the results of fitting data of the four zones in the joint, which is in good agreement with the OCP results.

Table 4. Fitting data of the four parts

Different regions of the welded joints	BM	FZ	HAZ	WZ
$E_{\text{corr}}/ \text{V}$	-0.89548	-0.77917	-0.77066	-0.7179
$I_{\text{corr}}/ \text{A} \cdot \text{cm}^{-2}$	8.81454×10^{-7}	0.1462513×10^{-7}	9.33899×10^{-7}	0.605759×10^{-7}

Fig. 6 exhibits the Nyquist plots of all zones of 7A52 Al alloy welded joint immersing in nature seawater for various periods, and the impedance data can be analyzed by equivalent circuit model [15]. An equivalent circuit model is given in Fig. 7, which was proposed to describe the corrosion behavior of TMW 7A52 Al alloy joint in natural seawater. The physical meanings of the equivalent circuit elements are as follow: R_s is the ohmic resistance of the electrolyte; C_f is the capacitance of the film; R_f is the pore resistance of the film; C_p is the capacitance of the double layer of each specimen; R_p is the polarization resistance of the electrode. It is generally believed, for a metallic system involving oxide film formation is concerned, that a system with higher R_p is less susceptible to be charged and has higher resistance to corrosion [16]. According to Fig. 8, the corrosion resistance of BM was the highest after immersing in seawater for 2 h and decreased minimum after immersing in nature seawater for 80 h which fits the change trend of corrosion potential. The R_p of BM and FZ are higher than WZ and HAZ before immersing for 200 h. After that, the corrosion resistance of BM, WZ, HAZ turned to be stable, and the magnitude is nearly same. However, R_p of FZ is larger than these three parts.

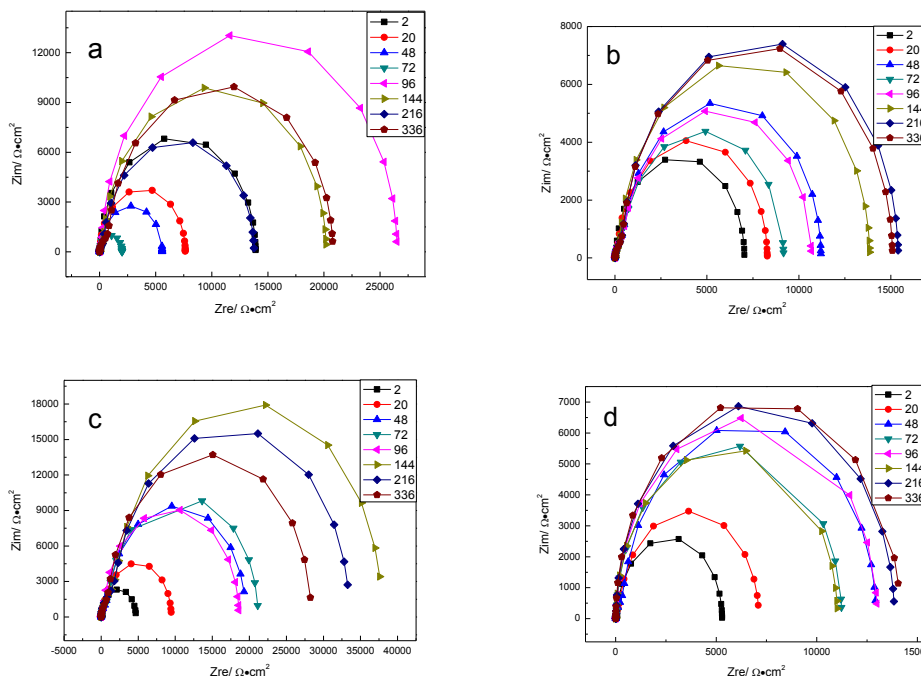


Figure 6. EIS of the specimens immersed in nature seawater for various periods:(a) BM,(b) WZ,(c) FZ,(d) HAZ.

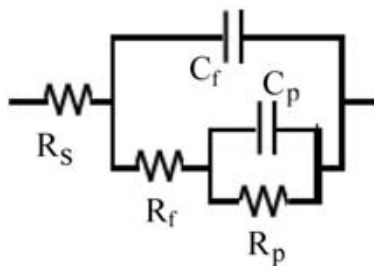


Figure 7. Equivalent circuit modeling of EIS.

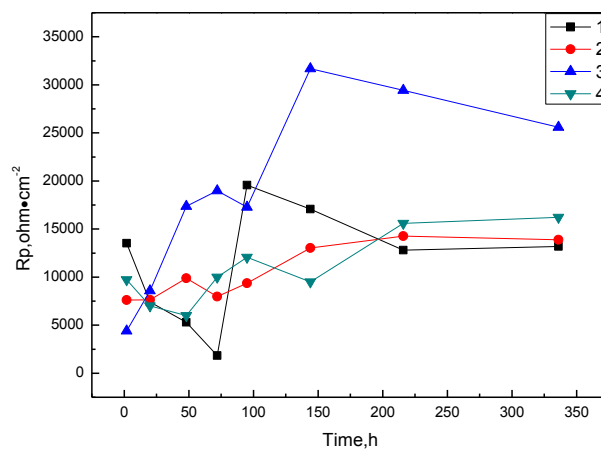


Figure 8. Polarization resistance (R_p) of the specimens: (1) BM, (2) WZ, (3) FZ, (4) HAZ.

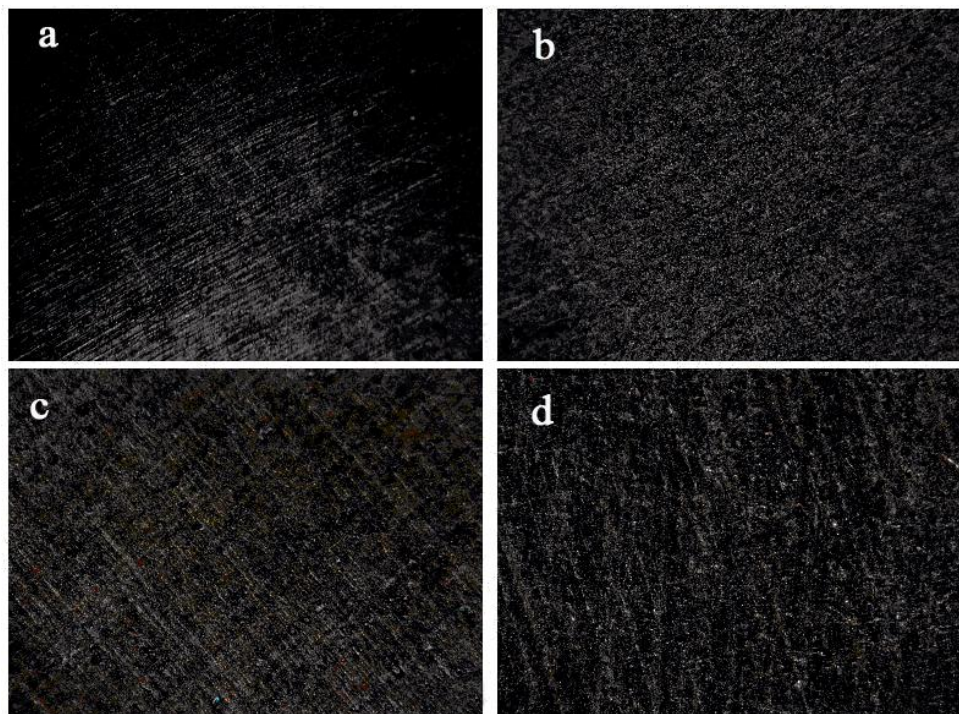


Figure 9. Macrograph of the specimens immersed in seawater after 200h: (a) BM, (b) WZ, (c) FZ, (d) HAZ.

Moreover, Fig. 9 showed the macrograph of the TMW specimens immersed in seawater for 200 h. Examining photographs shown in Fig. 9, it was found that the WZ and HAZ corroded seriously compared to BM and FZ which agrees with the results from impedance data analysis. However, the corrosion resistance of WZ and HAZ is approximate comparing with that of BM immersed for 200 h. It indicated the WZ and HAZ of 7A52 Al alloy joint become more resistance to corrosion after immersing for 200 h, which was attributed to the uniform distribution of secondary phase particles and the fine grain size found in this region [9].

4. CONCLUSION

(1) Microstructure of welded joint of 7A52 Al alloy included four zones, that is, base metal, thermo mechanically affected zone, fusion zone and weld zone. Different amounts of zinc and magnesium element in the joint led to M-type distribution of hardness.

(2) The open-circuit potential of BM was slightly negative, but it exhibited good corrosion resistance due to the protection of the oxide film on the surface. FZ had the best corrosion resistance among the four specimens, the corrosion resistance of WZ and TMAZ became better than ever and then turned to be stable along with immersing process.

References

1. J. W. Huang, Z. M. Yin, X. F. Lei, *Transactions of Nonferrous Metals Society of China*, 18(2008) 804-808.

2. K. Nishimoto, K. Ogawa, *Welding international*, 13(1999) 845-854.
3. T. G. Gooch, *Welding Journal-Including Welding Research Supplement*, 75(1996) 135s.
4. Z. Fang, Y. Wu, R. Zhu, *Corrosion*, 50(1994) 171-175.
5. L. Y. Xu, M. Li, H. Y. Jing, Y. D. Han, *Int. J. Electrochem. Sci.*, 8(2013) 2069-2079.
6. N. Winzer, A. Atrens, W. Dietzel, *Materials Science and Engineering: A*, 488(2008) 339-351.
7. M. Popović, E. Romhanji, *Journal of materials processing technology*, 125(2002)275-280.
8. S. Katsas, J. Nikolaou, G. Papadimitriou, *Materials & design*, 28(2007)831-836.
9. M. B. Kannan, W. Dietzel, R. Zeng, *Materials Science and Engineering: A*, 460(2007)243-250.
10. X. Wang, R. Jia, H. Zhang, H. Liu, *Advanced Materials Research*, (2011)311-313.
11. S. H. C. Park, Y. S. Sato, H. Kokawa, *Scripta Materialia*, 49(2003) 161-166.
12. J. C. Lin, H. C. Shih, *Journal of the Electrochemical Society*, 134(1987) 817-823.
13. D. Battocchi, A. M. Simoes, D. E. Tallman, *Corrosion science*, 48(2006) 1292-1306.
14. S. J. Kim, S. K. Kim, J. C. Park, *Surface and Coatings Technology*, 205(2010) S73-S78.
15. S. A. McCluney, S. N. Popova, B. N. Popov, *Journal of the Electrochemical Society*, 139(1992) 1556-1560.
16. J. C. Lin, H. L. Liao, W. D. Jehng, *Corrosion Science*, 48(2006)3139-3156.